

Inter-Vehicle Channel Modeling at 60 GHz Frequency Band

Meysam Shadbakhsh¹, Ali Shahzadi²

1- Department of Electrical Engineering, Shahre-Rey Branch, Islamic Azad University, Tehran, Iran
Email: Me.Shadbakhsh@gmail.com

2- Department of Electrical Engineering, Shahre-Rey Branch, Islamic Azad University, Tehran, Iran
Email: shahzadi@iust.ac.ir

Received: Nov. 22 2013

Revised: Dec. 16 2013

Accepted: Feb. 1 2014

ABSTRACT:

In recent years, Inter-vehicle communication (IVC) has received great attention due to its many advantages such as public safety and reduction of accidents, traffic management, video and audio transmission between vehicles. Also, the 60 GHz frequency band with 7GHz bandwidth is good for video and audio transmission with HD quality and high data rate transmission (Gbps). But design of Communication systems need suitable channel model that is as simple and accurate as possible. In this paper, we propose vehicle-to-vehicle (V2V) channel model in 60 GHz Band. This model is combination of ray-tracing and cluster-based scattering models and its structure based on tapped delay line. In addition to geometry and material of environment, proposed model can also model Doppler spectrum of both mobile and stationary scatterers.

KEYWORDS: V2V, 60 GHz, Channel modeling, TDL, Doppler spectrum, Frequency selective channel.

1. INTRODUCTION

Inter-vehicle communication (IVC) is one of the most important components of intelligent transportation system (ITS). These systems enable communication between two vehicles in a single-hop when they are in the case of direct line of sight (LOS) and are in communication range. Or even these two vehicles aren't in the case of LOS nor in communication range, it enables multi hop communication between these vehicles. Some of the main advantages of such systems include public safety and reduction of accidents, traffic management, video and audio transmission between vehicles [1].

In recent years, public tendency for using services with very high rate to supporting high-definition audio and video transmission services has increased [2]. However, the 60 GHz frequency band with 7GHz bandwidth is available for unlicensed use in worldwide. This band is suitable for high- data rate transmission (Gbps) in short range.

Unlike other channels, providing such services in wireless environment faces strong challenges such as fading especially in variable environment and dynamic vehicle-to-vehicle (V2V).

However, communication systems need suitable channel model. A good radio channel model can provide detailed insight into the complex radio wave propagation mechanisms as well as allowing study of the achievable performance from both theoretical and simulation standpoints. In other hand, the mechanisms

that govern radio propagation in a wireless communication channel are very complex and diverse, which makes channel modeling interesting as a research subject. While it is important to keep the channel models as accurate as possible in order to sufficiently capture the key channel effects, the models developed must also be simple enough to be implemented. Hence, a good channel modeling approach involves a tradeoff between accuracy and simplicity of the system under investigation.

In this paper, regarding the unique features of 60 GHz frequency bands in high data transmission, we present a model for simulation of channel for inter-vehicle (V2V) applications.

The remainder of this paper is organized as follows: In Section 2, we briefly study specification of 60GHz band. In Section 3, we propose a combination model for V2V channel in 60 GHz band. In Section 4, we simulate the model. Finally, in last section, we conclude the paper and summarize the key findings.

2. SPECIFICATION OF THE 60GHZ BAND

The 60 GHz frequency band with 7GHz bandwidth is available for unlicensed use of wireless communication in worldwide. This band is good for high-data rate transmission (Gbps) in short range. In comparison with other unlicensed bandwidth allocated for ultra-wideband (UWB) purposes, the 60 GHz bandwidth is continuous and less restricted in terms of power limits [3]. In the following, some of advantages and

challenges associated with these bands are noted:

* **Millimeter wave length:** This millimeter wave ($\lambda = 5mm$) permits multiple-antenna solutions which could be unavailable at lower frequencies. The form factor of mm-wave systems is approximately 140 times smaller [3].

* **Free space path loss:** The path loss at 60 GHz is much more severe than at lower frequencies in a way which free space path loss at 60 GHz increases by approximately 22 dB compared to 5 GHz band [3].

* **Losses due to oxygen absorption and rain:** In addition to free space loss, path loss in 60GHz includes additional losses due to oxygen absorption and rain. The oxygen absorption peaks at 60 GHz with 15 dB attenuation per kilometer, while rain attenuation adds losses of a few decibels, depending on the rain intensity [3].

* **Frequency reusing:** the noted losses are also an advantage since they can increase frequency reusing, in a way which if the distance of links are about 4 Km, same frequency can be reuse [4].

* **First-order reflection:** at 60GHz band we can neglect second-order reflection [5] and only consider first-order reflection.

3. MODELING THE CHANNEL

In this section, we propose a combined model to modeling of V2V channel at 60 GHz Band. This model is combination of ray-tracing and cluster-based scattering models. In this model, we first use ray-tracing model process power delay profile (PDP) in receiver location, and then account statistical properties according to the each stationary and mobile scatterers properties. In the following we will describe each of the models used.

3.1. Ray-tracing model

This model is based on the mechanism of propagation of electromagnetic waves, such as free space propagation, reflection, diffraction and scattering and need to describe each geometry, position and scattering properties of environment objects. Classical ray tracing determines all rays that can go from one TX location to one RX location. The method operates in two steps [6]: 1. First, all rays that can transfer energy from the TX location to the RX location such as LOS ray and other multipath rays are determined. This is usually done by means of the image principle. 2. In a second step, attenuations (due to free space propagation and finite reflection coefficients of each paths including earth, moving objects and fixed objects) are computed. Then power and delay of rays can be determined using electromagnetic waves equations. Ray tracing allows fast computation of single- and double-reflection processes.

3.1.1. Path loss

Path loss describes the attenuation of signal and is defined by (1) [7]:

$$L = \left(\frac{P_t}{P_r} \right) = \left(\frac{(4\pi)^2 R^2}{G_t G_r \lambda^2} \right) \quad (1)$$

where L is propagations loss in free space, P_t and P_r are transmitted and received powers, G_t and G_r are gain of the transmitting receiving antenna, respectively. R is path length of ray, and λ is wavelength Proportional to operating frequency. When gain of antenna is neglected and suppose they are unit, expression can be simplified as follows:

$$L = \left(\frac{P_t}{P_r} \right) = \left(\frac{4\pi R}{\lambda} \right)^2 \quad (2)$$

3.1.2. Atmospheric loss

Atmospheric loss due to oxygen, K , in the 60 GHz band is equal to 15dB/Km and is considered by following expression:

$$K = 10^{15R/10000} \quad (3)$$

3.1.3. The received signals

Receiving signal E at receiver antenna for line of sight (LOS) path can be expressed as follows [8]:

$$E_{LOS} = \sqrt{P_r} \cdot e^{-j\phi} = \sqrt{\frac{G_{t,LOS} G_{r,LOS}}{LK}} P_t \cdot e^{-j\beta R} \quad (4)$$

where $G_{t,LOS}$ and $G_{r,LOS}$ are gain of the transmitting receiving antenna in the LOS path, respectively and ϕ is phase delay defined by the propagation constant, β and R . Also, receiving signals of other paths (included of reflected signals from the ground and other surfaces) can be expressed as follows:

$$E_r = \sum_{k=1}^N \Gamma_k \sqrt{\frac{G_{t,k} G_{r,k}}{L_k K_k}} P_t \cdot e^{-j\beta R_k} \quad (5)$$

where N is number of reflected multi-paths from other surfaces, $G_{t,k}$ and $G_{r,k}$ are gain of the transmitting receiving antenna, respectively, L_k is path loss, K_k is atmospheric loss, R_k is path length corresponding of k th path.

3.1.4. The received signals

Γ is complex reflection coefficient of surface and are expressed for horizontal and vertical polarization respectively as follows [9]:

$$\Gamma_h = \frac{\cos(\theta_i) - \sqrt{n^2 - \sin^2(\theta_i)}}{\cos(\theta_i) + \sqrt{n^2 - \sin^2(\theta_i)}} \quad (6)$$

$$\Gamma_v = \frac{n^2 \cos(\theta_i) - \sqrt{n^2 - \sin^2(\theta_i)}}{n^2 \cos(\theta_i) + \sqrt{n^2 - \sin^2(\theta_i)}} \quad (7)$$

where n is complex refractive index and θ_i is incident angle on surface. For any surface are different n . for example, complex refractive index of road surface paved with asphalt is $2-j0.05$ [9]. Because this small value of n for road surface paved with asphalt, vertically polarized wave is smaller than a horizontally polarized wave. Since in the V2V communication, after the LOS signal, reflected signal from road is main received signal, thus, the use of vertically polarized wave has advantages for V2V communication in term of stability of received power, in comparison with that horizontally polarized wave.

3.1.4. Effect of undulating road

In [10] effect of undulating road is calculated and measured. Results show that received power in LOS case can be obtained by superimposition the fluctuation, which follows a logarithmic normal distribution, due to undulation in road on the value defined by the two-ray model on a flat surface.

3.2. Modeling of multipath power-delay profiles with tapped-delay line (TDL)

For Modeling of multipath power-delay profiles of a frequency selective channel Some methods have been proposed [11] that include : method of equal distances (MED), mean-square-error method (MSEM), method of equal areas (MEA), Monte-Carlo method (MCM), and L^p -norm method (LPNM). The LPNM method has best performance but has need complex calculations. In this section, we use the MED method that has acceptable performance.

3.2.1. Multipath power-delay profiles of simulation model

The tapped-delay line channel simulator considered here is characterized by the following expression [11]

$$\tilde{h}(\tau, t) = \sum_{l=0}^{L-1} \tilde{a}_l \tilde{\mu}(t) \delta(\tau - \tilde{\tau}_l) \quad (8)$$

Where L is the number of paths with different propagation delays, $\tilde{\tau}_l$ are discrete propagation delays, the real-valued coefficients \tilde{a}_l are path gains, and

$$\tilde{\mu}_l(t) = \tilde{\mu}_{1,l}(t) + j\tilde{\mu}_{2,l}(t) \quad l = 0, 1, \dots, L-1 \quad (9)$$

is a stochastic process where is determined with given spectral shapes (Doppler power spectra). The equivalent complex baseband structure of the simulator for the frequency-selective channel model with the impulse response described by (8) is shown in Figure 1. In this figure, $x(t)$ is the input signal, $y(t)$ is the resulting output signal, and $\Delta\tilde{\tau} = \tilde{\tau}_l - \tilde{\tau}_{l-1}$ ($l = 0, 1, \dots, L-1$) stands for the delay difference between the propagation paths

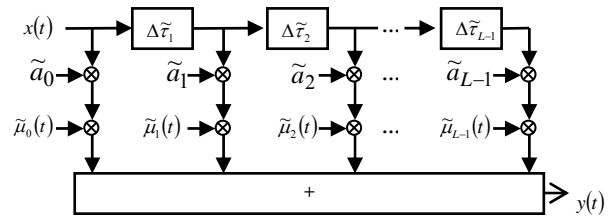


Fig. 1. Tapped-delay line model for a frequency-selective fading channel in the equivalent complex baseband [11]

l and $l-1$. Since the value of the first propagation delay $\tilde{\tau}_0$ has no effect on the behavior of the simulation model, it has been set to zero for convenience.

It has been shown that Multipath power-delay profile $\tilde{S}_\tau(\tau)$ of the tapped-delay line channel simulator can be expressed by

$$\tilde{S}_\tau(\tau) = \sum_{l=0}^{L-1} \tilde{a}_l^2 \delta(\tau - \tilde{\tau}_l) \quad (10)$$

With respect to the expression (10) and knowing the parameter sets $\{\tilde{\tau}_l\}_{l=0}^{L-1}$ and $\{\tilde{a}_l\}_{l=0}^{L-1}$, we can be obtained the multipath power-delay profile model for simulation aims.

3.2.2. MED method

Let $S_\tau(\tau)$ be any given specified multipath power delay profile characterized by the fact that is equal to zero outside the interval $I = [0, \tau_{\max}]$ [11]. Then, the discrete propagation delays $\tilde{\tau}_l$ are defined by multiples of a constant quantity $\Delta\tau$ according to

$$\tilde{\tau}_l = l\Delta\tau \quad l = 0, 1, \dots, L-1 \quad (11)$$

Where $\Delta\tau$ is related to τ_{\max} and $L > 1$ according to $\Delta\tau = \tau_{\max} / (L-1)$. Also path gain can be calculated through the following expression:

$$\tilde{a}_l = \sqrt{\int_{\tau \in I_l} S_\tau(\tau) d\tau} \quad l = 0, 1, \dots, L-1 \quad (12)$$

3.3. Doppler models

Modeling of Doppler spectra in V2V communication channel is one of the major problems in the description of the vehicular networks. The movement in wireless channel cause Doppler shift in the received signal as a function of the angle between the signal path and direction of motion. Signals arrived at receiver after experiencing reflections from scatterers. Superposition of these multipath components with range of Doppler shifts and received powers represents a Doppler spectrum at receiver. The exact shape of the Doppler spectrum is a function of the wireless environment.

3.3.1. Experimental results

Figure 2 shows example of the observed experimental Doppler spectra in the V2V environment [12]. This spectrum can be generally decomposed into three components:

- 1) The first and strongest component is that from line-of-sight (LOS). This component exhibits a Doppler shift proportional to the relative velocity, but no Doppler spreading.
- 2) The second component is a weaker, roughly continuous base and arises from stationary scattering sources.
- 3) Finally, additional features are observed beyond the base including narrow, shifted peaks and broadened base structures. These features result from moving scattering objects in the environment, particular vehicles in the oncoming lanes.

Then, in real condition, Doppler spectrum is highly variable and even can be having out-of-band peak $(-f_m, f_m)$. Doppler spectrum depends on the relative speed and distance between vehicles, road traffic conditions and properties of road. Also, antenna radiation pattern at transmitter/receiver array can be depends on elevation and azimuth angles.

3.3.2 Models of stationary scatterers

In the reference models of Wireless Access in Vehicular Environment (WAVE), with matching data of channel listening tests, the following models are considered for stationary objects Doppler models in V2V environment. Figure 3 illustrates these spectrums [13]. The (unnormalized) Doppler power spectral density (dpsd) functions for the JakesX, round, and flat spectrum shapes respectively are:

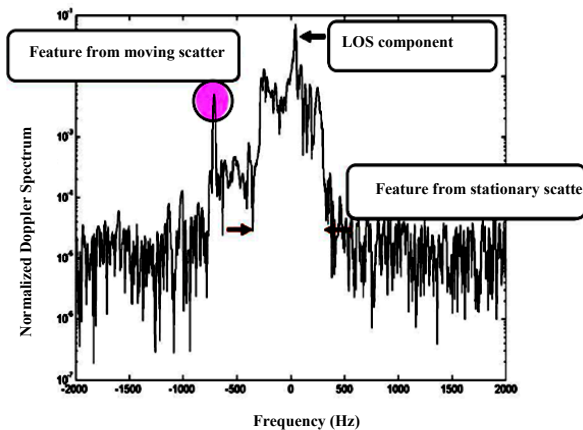


Fig. 2. Sample of the observed experimental Doppler spectra in the V2V environment (SISO channel) [12]

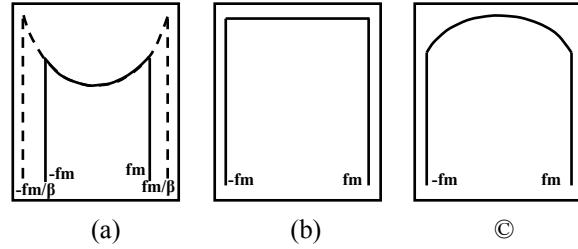


Fig. 3. Doppler spectrums models of stationary scatterers (a)JakesX, (b)Flat , (c)Round

$$S_{jakesX}(f_D) = \begin{cases} \frac{\beta}{\pi f_m \sqrt{1 - \left(\frac{\beta f_D}{f_m}\right)^2}} & |f_D| \leq f_m \\ 0 & otherwise \end{cases} \quad (13)$$

$$S_{round}(f_D) = \begin{cases} \pi f_m \sqrt{1 - \left(\frac{f_D}{f_m}\right)^2} & |f_D| \leq f_m \\ 0 & otherwise \end{cases} \quad (14)$$

$$S_{flat}(f_D) = \begin{cases} 1 & |f_D| \leq f_m \\ 0 & otherwise \end{cases} \quad (15)$$

Where $f_m = \frac{V_T}{\lambda} + \frac{V_R}{\lambda}$ is the maximum Doppler shift and

$\beta = \sqrt{1 - 10^{-X/5}}$ where $X \geq 0$ is in dB (thus $0 \leq \beta \leq 1$). The JakesX spectrum becomes the classic Jakes spectrum as $X \rightarrow \infty$ or equivalently $\beta \rightarrow 1$.

3.3.3. Models of mobile scatterers

For modeling the mobile scatterers, we use the proposed model in [14]. The main advantage of this model is that it takes into account the impact of cluster-based scattering of waves and directivity of antennas on the Doppler spectrum. In this model, suppose that there are N separate clusters, and each cluster contributes to the total received energy according to a given weight factor, which is a measure of multipath power relative to the power of the strongest path. If we denote the angular density and the power weight of the n_{th} cluster ($1 \leq n \leq N$) by $P_n(\theta, \phi)$ and w_n , respectively, and with considering the special condition of channel in V2V environment such as Rician distribution for signal variations in LOS case and sparse road traffic, low elevation antennas and ... , with execution of angle of arrival (AOA), It has been shown diffuse Doppler spectrum can be written as

$$S(f) = \xi \sum_{n=1}^N w_n \left[\int_{\Omega(f)} \frac{\Gamma_n(\theta, \omega; \phi_n, \kappa_n, \epsilon_n)}{f_{max} \cos(\omega)} d\theta + \int_{\Omega(f)} \frac{\Gamma_n(\theta, \pi - \omega; \phi_n, \kappa_n, \epsilon_n)}{f_{max} \cos(\omega)} d\theta \right] \quad (16)$$

Where $\Omega(f) = \arcsin(|f|/f_{max})$ and $\Gamma_n(\theta, \varphi; \phi_n, \kappa_n, \epsilon_n)$ represents the n th cluster pattern which is the product

of antenna pattern and the nth cluster AoA pdf.

$$\Gamma_n(\theta, \varphi, \phi_n, \kappa_n, \varepsilon_n) = U(\theta, \varphi) P_{\Theta_n}(\theta; \varepsilon_n) P_{\Phi_n}(\varphi; \phi_n, \kappa_n) \quad (17)$$

and the constant factor ξ is given by

$$\xi = \frac{G_T P_T L}{(K + 1) \times \sum_{n=1}^N w_n} \quad (18)$$

where G_T is P_T represent the Tx antenna gain and the transmitter power, respectively. L represents the total propagation loss, K denotes the Rician k-factor, $U(\theta, \varphi)$ is the receiving antenna radiation intensity. Also, $P_{\Phi_n}(\varphi)$ and $P_{\Theta_n}(\theta)$ are azimuth AoA and the elevation AoA of n_n cluster and suppose that they are statistically independent.

a) For azimuth AOA

It has been shown that the von Mises pdf is an eligible distribution for the azimuth AoA. By definition we have:

$$P_{\Phi_n}(\varphi; \phi_n, \kappa_n) = \frac{\exp[\kappa_n \cos(\varphi - \phi_n)]}{2\pi I_0(\kappa_n)}, \quad 0 \leq \varphi < 2\pi \quad (19)$$

Where $I_0(\cdot)$ is the zeroth-order modified Bessel function of the first kind. Parameters ϕ_n and κ_n determine the mean and the spread for the n_n cluster in the horizontal plane, respectively. Experimental results show that the multipath rays due to mobile clusters are associated with small azimuth spread, or equivalently, very large values of κ_n . It has been shown that for very large values of κ_n , the von Mises pdf becomes a Gaussian pdf with mean ϕ_n and variance $1/\kappa_n$. Hence, for modeling the effect of mobile clusters, we use the following pdf:

$$P_{\Phi_n}(\varphi; \phi_n, \kappa_n) = \frac{1}{\sqrt{2\pi/\kappa_n}} \exp\left[-\frac{(\varphi - \phi_n)^2}{2/\kappa_n}\right], \quad 0 \leq \varphi < 2\pi \quad (20)$$

For expressway scenario with low vehicular traffic density and oncoming RX and TX vehicles, κ_n due to vehicle scatterers has been reported between 1200-2500 and also For scenario when the RX and TX vehicles are traveling along the street surface with significant urban canyon effect, κ_n due to vehicle scatterers has been reported between 220-2500 [14].

b) For elevation AOA

In addition, former studies on mobile propagation channels in urban environments show that for low elevation antennas, as in the case of inter-vehicle communications, multipath signals arrive within a limited range in the elevation plane [14]. Thus, we neglected effect of this dimension in modeling.

4. SIMULATION OF THE MODEL

In this Section, we simulate the model of V2V channel at 60GHz band. First, we implement ray-tracing model and apply MED method to obtain tapped delay line (TDL) model. Then, we take in Doppler Effect using cluster-based scattering model. It is notable that we used MATLAB software for simulation.

For channel simulation, we firstly plan the scenario as follows. Suppose that TX and RX vehicles are travelling with velocity of $V_T = 30m/s$ and $V_R = 30m/s$, respectively, in same direction and in expressway with width of $W_s = 20m$. TX and RX antenna are Omni-directional and heights of TX and RX antenna from ground are $h_T = 0.49m$ and $h_R = 0.43m$, respectively. We suppose that there exists the line of sight (LOS) path. It's also that assumed that there are some vehicles around the TX and RX vehicles moving with velocity of v_s in same/opposite direction.

Figure 4 shows a typical V2V environment.

Figure 5(a) illustrate a multipath power-delay profile of V2V channel for LOS case with regard to surface reflections and number of $N=10$ scatterers. Relying on these results we can calculate RMS delay spread and coherence bandwidth. In this case, RMS delay spread and coherence bandwidth [15] are $\sigma_\tau = 4.9855 \times 10^{-9} s$ and $B_c = 1/50\sigma_\tau = 4.0111 \times 10^6 Hz$, respectively. Thus, the channel is frequency selective. Also, the Rician k-factor is computed 1.4571. Figure 5(b) illustrate simulation model by applying the MED with $L=5$.

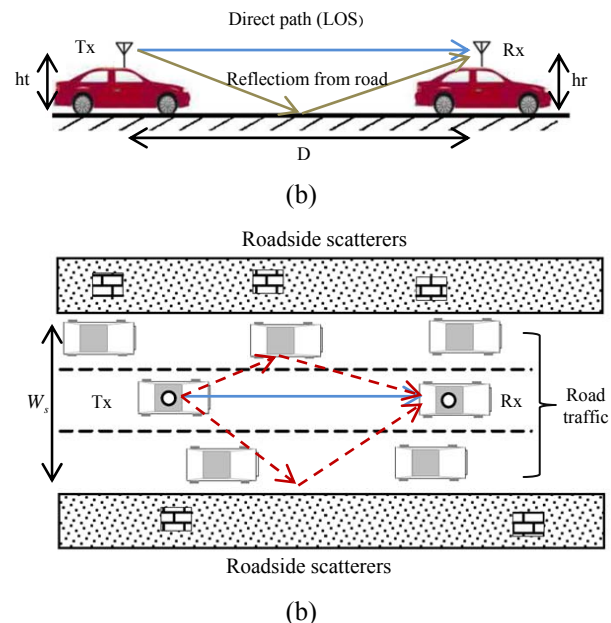


Fig. 4. A typical V2V environment and different signal paths (a) sidelong perspective (b) upside perspective

The maximum Doppler frequency of moving scatterers is $f_m = 2((V_T + V_S)/\lambda) = 24\text{KHz}$ due to the movement of scatterers in the opposite direction TX/RX. Also, the maximum Doppler frequency of stationary scatterers is half of the above value. Figure 6 show the theory and simulation Doppler spectrum with number of 5 path (tap) in which the Rician channel model is assumed. In this figure, Doppler spectrum of Tap1 due to stationary scatterers is simulated with Jakes model, while, Doppler spectrum of other taps due to moving scatterers are simulated with Bi.Gaussian model specified with central Doppler frequency proportional to the vehicles speed and the large variance. In each of these figures, the first Doppler spectrum, represented by the dashed red line, is a theoretical spectrum used in the multipath channel model. Note that the plotted Doppler spectrum is normalized to have a total power of 1. The second Doppler spectrum, represented by the blue dots, is determined by measuring the power spectrum of the multipath fading channel as the model generates path gains. Also, with respect to maximum Doppler frequency of $f_m = 2((V_T + V_S)/\lambda) = 24\text{KHz}$, we can calculate coherence time of the channel [15] as $T_c \approx 9/(16\pi f_m) = 7.4604 \times 10^{-6} \text{ s}$, so because of the high transmission rate in 60GHz, we expected slow fading channel in this case.

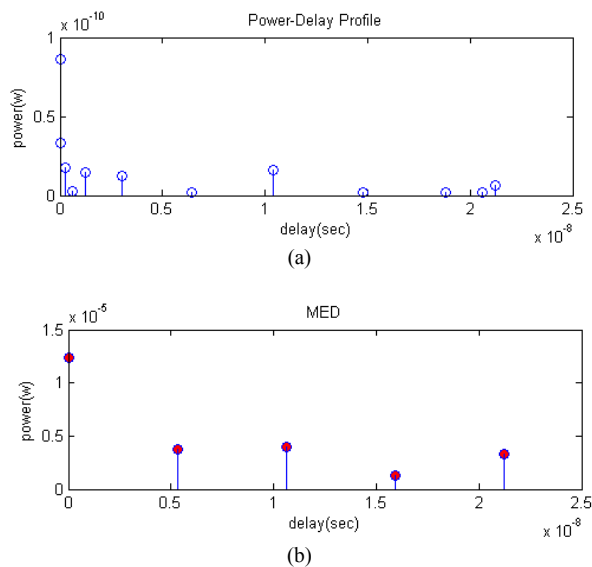


Fig. 5. (a) Multipath power delay profile $S_r(\tau)$ in 60GHz Band, (b) illustration of applying the MED with $L=5$

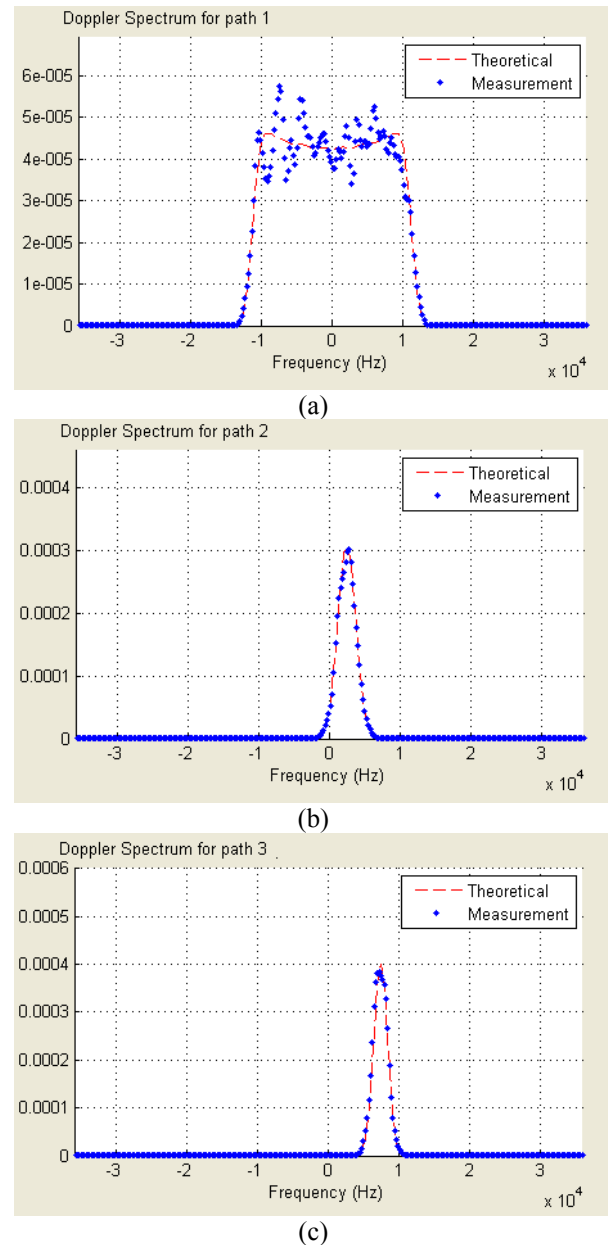


Fig. 6. The theory and simulation Doppler spectrum with number of 5 paths (taps) in which the Rician channel model is assumed (The plotted Doppler spectrum is normalized to have a total power of 1). (a)Tap1, (b)Tap2, (c)Tap3

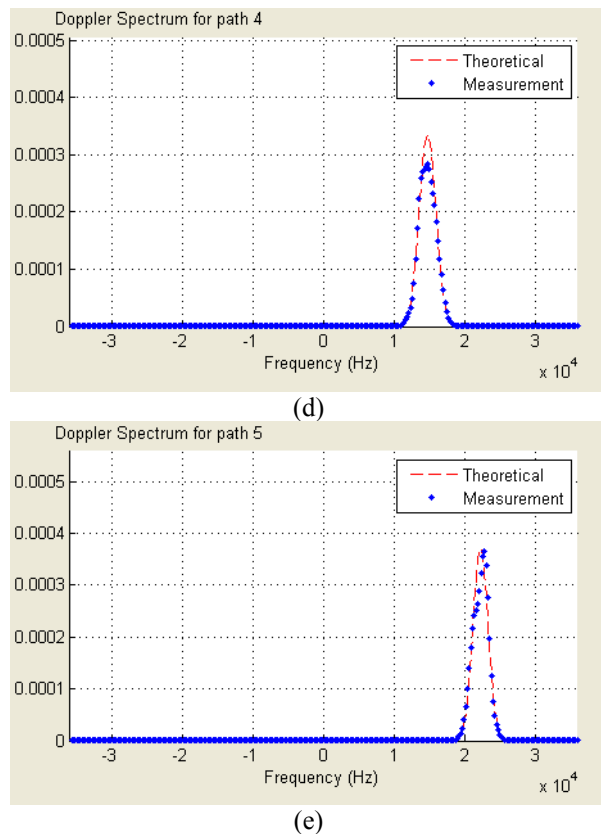


Fig. 6. Continue, (d)Tap4, (e)Tap5

These results indicate very special and variable conditions of V2V channel about which we have to think about solutions to deal with. The most suitable of these solutions is usage of multi antenna structures, especially method of space-time diversity and MIMO coding.

5. CONCLUSION

In this paper, we first studied the specification of 60GHz band and its unique features to data transmission with very high rate (Gbps) in short range communication. We then proposed a combination model for V2V channel in 60 GHz band with using combination of ray-tracing and cluster-based scattering models based on tapped delay line structure. We observed that in addition to geometry and material of V2V environment, it can model Doppler Effect of scatterers in a way which for stationary and moving scatterers are appropriate Jakes and Gaussian models, respectively. Moreover, other advantage of this model is that it takes into account the impact of directivity of antennas on the Doppler spectrum. The findings indicate that V2V channel is a slow-frequency selective channel and we have to think about some solution such as method of space-time diversity and MIMO coding to counteract its destructive effects and increase the reliability.

REFERENCES

- [1] Sichitiu, Mihail L., and Maria Kihl. "Inter-vehicle communication systems: a survey." *Communications Surveys & Tutorials, IEEE*, 10. 2, pp. 88-105, 2008.
- [2] Raychaudhuri, Dipankar, and Narayan B. Mandayam. "Frontiers of wireless and mobile communications." *Proceedings of the IEEE*, 100.4, pp. 824-840, 2012.
- [3] Yong, Su-Khiong, Pengfei Xia, and Alberto Valdes-Garcia. *60GHz Technology for Gbps WLAN and WPAN: From Theory to Practice*. Wiley, 2011.
- [4] Federal Communications Commission. "Millimeter wave propagation: spectrum management implications." Bulletin 70 (1997).
- [5] Maltsev, Alexander, et al. "Experimental investigations of 60 GHz WLAN systems in office environment." *Selected Areas in Communications, IEEE Journal on* 27.8, pp. 1488-1499, 2009.
- [6] Molisch, Andreas F. *Wireless communications*. Vol. 15. Wiley, 2010.
- [7] Rappaport, Theodore S. "Wireless communications: principles and practice". Vol. 2. New Jersey: Prentice Hall PTR, 1996.
- [8] Warren, L. Stutzman, and A. T. Gary. "Antenna theory and design." *John Wiley & Sons, New York*, pp. 76-171, 1998.
- [9] Mizutani, Katsuya, and Ryuji Kohno. "Analysis of multipath fading due to two-ray fading and vertical fluctuation of the vehicles in ITS inter-vehicle communications." *Intelligent Transportation Systems, 2002. Proceedings. The IEEE 5th International Conference on. IEEE*, 2002.
- [10] Yamamoto, Atsushi, Koichi Ogawa, and Hiroshi Shirai. "Empirical Investigation of the LOS Propagation Characteristics on an Undulating Road for Millimeter Wave Inter-Vehicle Communication." *IEICE transactions on electronics* 90.9, pp. 1807-1815, 2007.
- [11] Patzold, Matthias, Arkadius Szczepanski, and Neji Youssef. "Methods for modeling of specified and measured multipath power-delay profiles." *Vehicular Technology, IEEE Transactions on* 51.5, pp. 978-988, 2002.
- [12] Cheng, Lin, et al. "Doppler component analysis of the suburban vehicle-to-vehicle DSRC propagation channel at 5.9 GHz." *Radio and Wireless Symposium, 2008 IEEE. IEEE*, 2008.
- [13] Dulmage, Jared, and Michael P. Fitz. "Non-isotropic fading channel model for the highway environment." *Vehicular Technology Magazine, IEEE* 2.4, pp. 12-18, 2007.
- [14] Seyedi, Younes, et al. "Simulation of Doppler spectrum for Vehicle-to-Vehicle communications channels with directive antennas." *Mobile and Wireless Networking (iCOST), 2012 International Conference on Selected Topics in. IEEE*, 2012.
- [15] Rappaport, Theodore S. *Wireless communications: principles and practice*. Vol. 2. New Jersey: Prentice Hall PTR, 1996.